

Contents lists available at ScienceDirect

# **BBA** - Biomembranes

journal homepage: http://ees.elsevier.com



# Influence of interfacial tryptophan residues on an arginine-flanked transmembrane helix

Sara J. Sustich, Fahmida Afrose, Denise V. Greathouse, Roger E. Koeppe II\*

Department of Chemistry and Biochemistry, University of Arkansas, Fayetteville, AR 72701, United States of America

#### ARTICLE INFO

# Keywords

Transmembrane helix unwinding Deuterium NMR Arginine Tryptophan GALA

#### ABSTRACT

The transmembrane helices of membrane proteins often are flanked by interfacial charged or aromatic residues that potentially help to anchor the membrane-spanning protein. For isolated single-span helices, the interfacial residues may be especially important for stabilizing particular tilted transmembrane orientations. The peptide RWALP23 (acetyl-GR<sup>2</sup>-AW(LA)<sub>6</sub>WLAR<sup>22</sup>A-amide) has been employed to investigate the interplay between interfacial arginines and tryptophans. Here we replace the tryptophans of RWALP23 with A5 and A19, to investigate arginines alone with respect to helix fraying and orientation in varying lipid bilayers. Deuterated alanines incorporated into the central sequence allow the orientation and stability of the core helix to be assessed by means of solid -state <sup>2</sup>H NMR in bilayers of DOPC, DMPC and DLPC. The helix tilt from the bilayer normal is found to increase slightly when R2 and R22 are present, and increases still further when the tryptophans W5 and W19 are replaced by alanines. The extent of helix dynamic averaging remains low in all cases. The preferred helix azimuthal rotation is essentially constant for all of the helices in each of the lipid membranes considered here. The alanines located outside of the core region of the peptide are sensitive to helical integrity. The new alanines, A5 and A19, therefore, provide new information about the length of the core helix and the onset of unraveling of the terminals. Residue A19 remains essentially on the central helix in each lipid membrane, while residues A3, A5 and A21 deviate from the core helix to an extent that depends on the membrane thickness. Differential unraveling of the two ends to expose peptide backbone groups for hydrogen bonding therefore acts together with specific interfacial side chains to stabilize a transmembrane helix.

# 1. Introduction

The folding of membrane proteins within lipid bilayers often is dominated by one or more  $\alpha$ -helical segments. Multiple helices may be connected by flexible loop regions that join the individual helices into a multi-helix bundle. In this arrangement, the interfacial residues where transmembrane helices begin or end become important for defining the overall membrane protein structure. Polar and aromatic amino acids are hypothesized to assist in anchoring helices to the polar lipid head groups at the membrane-aqueous interface [1]. Indeed, arginine and tryptophan residues at membrane interfaces or somewhat submerged, either alone or together, are important for the properties of potassium channels [2,3], a glucose transporter [4], human immunodeficiency virus envelope glycoprotein [5,6], Ras-like phosphate-binding loop GT-Pases [7], low-density lipoprotein receptor [8], chemotaxis receptors

[9] and thrombopoietin receptors [10], among other membrane proteins. While the principles for folding membrane proteins are complex, model experimental peptide systems and molecular simulations have proven useful for understanding the nature of protein-lipid interactions [11]. This article will address some of these principles for examples of transmembrane domains that possess arginine alone, tryptophan alone, or tryptophan and arginine together at the respective membrane interfaces while, importantly, a defined central membrane-spanning core helix is held constant.

The synthetic "GWALP" peptide model [12] was adapted from an original "WALP" peptide model [13]. The WALP23 model contains four interfacial tryptophan (W2, W3, W21, W22) residues that serve to anchor the transmembrane helix. Though these peptides were useful for a variety of experiments, including modulations of the lipid phase behavior and initial investigations of the helix tilt, their high dynamic averaging raises barriers for understanding single-residue mutations. The

Abbreviations: DLPC, 1,2-dilauroyl-sn-glycero-3-phosphocholine; DMPC, 1,2-dimyristoylphosphatidylcholine; DOPC, 1,2-dioleoyl-sn-glycero-3-phosphocholine; Fmoc, fluorenyl-methoxycarbonyl; TFA, trifluoroacetic acid; GALA, geometric analysis of labeled alanines; GWALP23, acetyl-GGALW(LA)6LWLAGA-[ethanol]amide; RMSD, root mean squared deviation. 
\* Corresponding author.

E-mail address: rk2@uark.edu (R.E. Koeppe)

sequence variant GWALP23 (acetyl-GGALW5(LA)6LW19LAGA) was discovered to have a well-defined transmembrane orientation, with lower dynamic averaging [14], stabilized in part by unraveling of the helix terminals at the membrane interface [15]. This peptide has only two interfacial tryptophan residues (W5 and W19) located on either side of the central helix of repeating leucine-alanine residues. Due to the hydrophobicity of the Leu-Ala repeats, the core of the peptide adopts strong  $\alpha$ -helical structure that spans the non-polar interior of a membrane [16]. The two tryptophan residues exhibit preferred locations near each polar lipid-water interface [16], thereby providing the peptide helix with a well-defined tilted transmembrane orientation within the bilayer that can be observed using solid-state NMR spectroscopy. These properties, along with the defined dynamic nature of GWALP23, allow for investigations of the effects of "guest" residue substitutions on the helix orientation, dynamics and terminal unraveling within membrane bilayers of differing thickness.

As previously mentioned, aromatic as well as charged amino acids are important for anchoring a transmembrane helix to the polar regions of a lipid bilayer. The interfacial interactions have been shown to affect the helicity toward the termini as well as the orientations of helices within different lipid membranes [15,17]. Lipid-bilayer thickness will play an additional role for the interactions. Thicker bilayers may stretch the proteins more, lowering the helix tilt angles and perhaps increasing the dynamic averaging of peptide helices. Another important stabilizing factor could be the helix fraying that will expose peptide backbone groups for intermolecular hydrogen bonding at membrane interfaces [17].

Deuterium-labeled alanine residues facilitate solid-state NMR experiments for measurement of the <sup>2</sup>H quadrupolar splittings and determination of the transmembrane helix integrity and orientation [15,18]. Typically, the <sup>2</sup>H-Ala residues are introduced in pairs within the core helix at 50% and 100% relative isotope abundance, to facilitate spectral assignment [14]. Additionally, the Ala residues 3 and 21 near each terminal of the peptide allow for investigations of the secondary structure at the ends of the sequence. It is therefore possible to examine whether the peptide ends are helical or frayed as well as how fraying affects peptide-lipid interactions.

Previous research investigated the tilt of the parent helix with tryptophans W5 and W19 and either glycines, G2 and G22, or arginines, R2 and R22 near the peptide terminals [14]. In both cases the helices showed well-defined transmembrane orientations with low dynamic averaging. Now we investigate the influence of removing the tryptophans, replacing them with A5 and A19, with arginines R2 and R22 present. Additionally, we label the juxta-terminal alanine residues (A3 and A21) to examine the potential unraveling of each helix, in the context of "only" tryptophan, "only" arginine, or both tryptophan and arginine, at the membrane interface. The three residue separation (2 versus 5, and 22 versus 19) for the candidate anchor residue placements are appropriate based on the known relative preferred locations for positively charged side chains as opposed to aromatic indole side chains at the membrane interface, an approximate 3-4 Å displacement [19]. Furthermore, when the tryptophans are absent from the sequence, the replacement alanines (A5 and A19) provide additional opportunities for deuterium labeling, leading to more detailed investigations of the central helix.

The results of this research are important for understanding the effects of single or double, cooperating or competing, interfacial "anchoring" residues for the properties of a well-defined transmembrane helix. The candidate peptides and their sequences are shown in Table 1, and a model of the basic molecular architecture with positions for  $^2$ H-alanine labeling is shown in Fig. 1. Each of the synthesized peptides was examined in oriented bilayers of DLPC, DMPC, and DOPC.

Table 1
Sequences of GWALP23-like peptides.

| Name   | Sequence  | Reference                 |
|--|---|---------------------------|
| GW <sup>5,19</sup> ALP23<br>RW <sup>5,19</sup> ALP23<br>RA <sup>5,19</sup> ALP23 | Ac-GG $^2$ ALW $^5$ L <u>ALALALALALALW</u> $^{19}$ LAG $^{22}$ A-amide Ac-GR $^2$ ALW $^5$ LALALALALALALAU $^{19}$ LAR $^{22}$ A-amide Ac-GR $^2$ ALA $^5$ LALALALALALALALA $^{19}$ LAR $^{22}$ A-amide | [14]<br>[14]<br>This work |

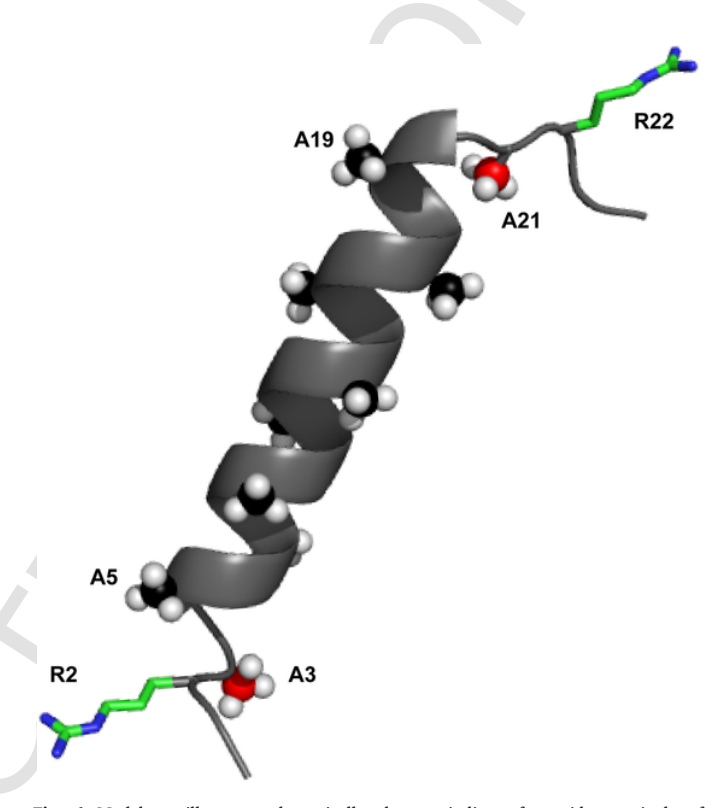


Fig. 1. Model to illustrate schematically the unwinding of peptide terminals of  $RA^{5.9}ALP23$  oriented in a DLPC bilayer, drawn using PyMol [20]. The side chains of arginines 2 and 22 are shown with green carbon atoms and blue nitrogen atoms. The alanine methyl groups available for deuterium labeling are shown as space filing, with the  $\beta$ -carbons colored black for core alanines A5 to A19 and red for the outer alanines A3 and A21.

#### 2. Materials and methods

Peptides were synthesized in solid phase on a 0.1 mmol scale, using an Applied Biosystems 433A Peptide Synthesizer from Life Technologies (Foster City, CA), with extended times for deprotection or coupling where needed. N-fmoc amino acids, including side chain protected Trp (boc group) and Arg (pbf group), were purchased from NovaBiochem (San Diego, CA), Anaspec (Fremont, CA), and Bachem (Torrence, CA). Deuterated alanines from Cambridge Isotope Laboratories (Tewksbury, MA) were manually derivatized with the N-fmoc protecting group, following the procedure described previously [21,22]. Each peptide was synthesized with two deuterated alanines differing in isotope abundance (50% and 100%  $d_{\rm 4}$ ) at particular positions, to distinguish and assign the  $^2{\rm H}$  signals observed by solid-state deuterium NMR spectroscopy.

After the completion of synthesis, peptides were cleaved from Rink amide resin at 22 °C for 3 h using an 85:5:5:5 solution of TFA:triiso-propylsilane:H $_2$ O:phenol (v/v; w/v for phenol). The cleavage mixture was filtered and peptide precipitated using methyl-t-butyl ether:hexane (50:50) and lyophilized several times from acetonitrile:water (50:50) to remove traces of solvent. Peptides were purified by reversed-phase HPLC on an octyl-silica column (Zorbax Rx-C8, 9.4  $\times$  250 mm, 5  $\mu m$ 

S.J. Sustich et al.

BBA - Biomembranes xxx (xxxxx) xxx-xxx

particle size) from Agilent Technologies (Santa Clara, CA) using a gradient of 90–94% (for RA $^{5,19}$ ALP) or 92–96% (for RW $^{5,19}$ ALP) methanol in water containing 0.1% TFA (v/v). Due to the absence of aromatic groups in RA $^{5,19}$ ALP23, the detector wavelength was set to 220 nm while purifying and quantifying this peptide, whereas the Trp-containing peptides were detected based on absorbance at 280 nm. The molecular masses and deuteration patterns were verified by MALDI-TOF mass spectrometry.

Mechanically aligned samples for solid-state NMR spectroscopy were prepared using 1.33 µmol peptide and 80 µmol lipid (1:60, mol:mol), using DLPC, DMPC, or DOPC phospholipids from Avanti Polar Lipids (Alabaster, AL), as described [18,23,24]. Initially, a peptide-lipid mixture was prepared from peptide dissolved in trifluoroethanol and lipid dissolved in chloroform. The solvents were removed under nitrogen flow followed by drying under vacuum. After dissolution in about 1 mL of 95% methanol/5% water (v/v), the mixture was distributed evenly over about 40 glass plates (4.8 × 23 × 0.07 mm; Marienfeld Laboratory Glassware, Lauda-Königshofen, Germany). Solvents were removed by drying under vacuum (≤ 0.010 Torr) for two days. The resulting peptide-lipid films were hydrated with deuterium-depleted water (Cambridge) to achieve 45% (w/w) hydration. The slides with the hydrated films were immediately stacked, sealed in a glass cuvette [18] and allowed to incubate for at least 48 h at 40 °C to achieve bilayer alignment. For confirmation of bilayer alignment within each sample by means of <sup>31</sup>P NMR, a wide-line probe (Doty Scientific, Columbia, SC) was employed with broad-band <sup>1</sup>H decoupling on a Bruker Avance 300 spectrometer. Deuterium (2H) NMR spectra were recorded at 50 °C using both  $\beta = 90^{\circ}$  (bilayer normal perpendicular to magnetic field) and  $\beta = 0^{\circ}$  macroscopic sample orientations, utilizing a quadrupolar echo pulse sequence [25] with full phase cycling, 105  $\mu s$  echo delay, 3.2  $\mu s$ pulse length and 120 ms recycle delay. Approximately 0.9 to 1.5 million free induction decays were recorded during each <sup>2</sup>H NMR experiment. An exponential weighting function with 100 Hz line broadening was applied prior to Fourier transformation.

For circular dichroism measurements, small unilamellar lipid vesicles with incorporated peptides (1:60, peptide:lipid, mol:mol) were prepared by sonication, with peptide concentrations of about 100  $\mu M$ . The spectra were recorded with a Jasco J-1500 spectropolarimeter, using a 1 mm cell path length, 1.0 nm bandwidth, 0.1 nm slit and 20 nm/min scan rate, and averaging ten scans.

The helix orientations, dynamic properties and unraveling of ends were analyzed by means of the semi-static GALA (geometric analysis of labeled alanines) method, taking the average tilt  $\tau_0$  of the helix axis, azimuthal rotation  $\rho_0$  about the helix axis and principal order parameter  $S_{zz}$  as variables [18,26]. We additionally employed a modified Gaussian approach [27] involving three variables,  $\tau_0$ ,  $\rho_0$  and  $\sigma_\rho$  (rotational slippage), with fixed values for  $S_{zz}$  and  $\sigma_\tau$  (helix wobble), as described previously [24].

# 3. Results

To examine the interactions of interfacial arginines, alone and with tryptophans, flanking the transmembrane segments of biological proteins and their possible roles with respect to the terminal fraying or the orienting of the helix axis in a lipid bilayer, we have employed derivatives of the established GWALP23 peptide framework [14,24]. Pairs of arginine residues were introduced to replace glycines 2 and 22 to give the sequence acetyl-GR<sup>2</sup>ALW<sup>5</sup>LALALALALALALALWI<sup>9</sup>LAR<sup>22</sup>A-amide (Table 1), which has been investigated in part by Vostrikov et al. [14,24] Then, for comparison, the tryptophan residues W5 and W19 were replaced with alanine residues (A5 and A19), to yield a peptide anchored only by arginine residues, R2 and R22. These substitutions also provide a longer aliphatic core and additional Ala residues for deuterium labeling, compared to the GWALP23 parent peptide (Table 1 and Fig. 1). We have addressed the influence of terminal arginine

residues, in the presence and absence of interfacial tryptophans, the length of the core helix, and the fraying of terminal residues.

The new analogue "RAALP23," acetyl-GR²ALASLALALALALALAI³9LAR²2A-amide (Table 1), lacking tryptophans, was synthesized successfully and its molecular mass was confirmed by MALDI-TOF mass spectrometry (Fig. S1). The circular dichroism spectra in several lipid bilayer membranes confirm a largely  $\alpha$ -helical secondary structure for RAALP23, with pronounced double minima near 208 nm and 222 nm (Fig. S2). When macroscopically oriented hydrated lipid-peptide samples were prepared, the bilayers were well aligned, as indicated by the  $^{31}P$  NMR spectra of the lipid head groups in the  $\beta=0^\circ$  and  $\beta=90^\circ$  sample orientations (Fig. S3).

Using <sup>2</sup>H solid-state NMR methods, we have deduced the average orientation and dynamic properties of the RAALP23 helix with respect to the lipid bilayer normal in DLPC, DMPC and DOPC membranes. Because the guanidinium group of Arg remains universally charged up to at least pH 13, as confirmed extensively [28–31,32], we hydrated the samples with unbuffered <sup>2</sup>H-depleted water. In this work we present the orientation analysis and potential unraveling of the RAALP23 helix and compare its properties with related membrane-spanning helices.

# 3.1. Orientation analysis of RAALP23 and RWALP23

The <sup>2</sup>H NMR spectra for the oriented samples of RAALP23 in lipid bilayers reveal defined sets of signals for the <sup>2</sup>H-labeled methyl groups of core alanines including A5 and A19 (Figs. 2 and S4). (Apart from the major symmetric pairs of peaks, minor peaks near zero kHz are attributed to natural-abundance deuterium in the water or lipids or occasionally to miss-oriented peptide components.) Focusing on the <sup>2</sup>H quadrupolar splitting magnitudes  $|\Delta\nu_q|$  of the central alanines 7, 9, 11, 13, 15 and 17 for RAALP23, we observe that this new helix displays a relatively large range of <sup>2</sup>H quadrupolar splitting magnitudes, from 7 to 35 kHz in DLPC, 5-28 kHz in DMPC and 5-23 kHz in DOPC. The wide ranges of  $|\Delta \nu_{\rm q}|$  values suggest a significant bilayer-dependent tilted orientation of the peptide helix with low dynamic averaging in each membrane. It is noteworthy that these magnitudes individually and as a range throughout the helix appear to be even larger in RAALP23 than in the related RWALP23 helix [14] in DLPC, DMPC, and DOPC bilayers. The results indicate similar well-ordered orientations with low dynamics for the RAALP23 and RWALP23 helices, with a somewhat larger helix tilt when tryptophan is absent at the bilayer interface (see below).

By replacing tryptophans 5 and 19 with  $^2H$ -labeled alanines, we were able to record signals and measure quadrupolar splittings for two additional alanine residues (Table 2). We addressed the helix orientation and dynamic properties using a semi-static GALA analysis [18,26] of the observed  $^2H$  quadrupolar splittings of the central six core alanine methyl side chains, to determine the lowest RMSD based on the helix tilt ( $\tau$ ), rotation ( $\rho$ ) and principal order parameter ( $S_{zz}$ ) as variables. Additionally, we treated the helix dynamics using a modified Gaussian analysis based on  $\tau_0$ ,  $\rho_0$ , and a distribution width  $\sigma_\rho$  as three variables, with a fixed  $\sigma_\tau$ , as described previously [24].

From the results of GALA analysis of the six central deuterated alanine methyl groups (Table 3), the quadrupolar wave plots (Fig. 4) indicate similar helix properties when the tryptophan residues W5 and W19 are removed. The azimuthal rotation appears to be similar between the helices with and without the tryptophans in all lipids, varying within only a small range from  $302^{\circ}$ - $318^{\circ}$  (Table 3). The  $S_{zz}$  values ranging from 0.70 to 0.86 indicate modest dynamic averaging. The helix tilt without tryptophans is about 4° larger for RAALP23 compared to RWALP23 in all lipids (Fig. 4; Table 3). While small, the difference in tilt is consistent and reproducible in each lipid membrane, thereby illustrating the high sensitivity of the  $^2$ H quadrupole splitting to small changes in molecular orientation. The similarity in dynamic averaging

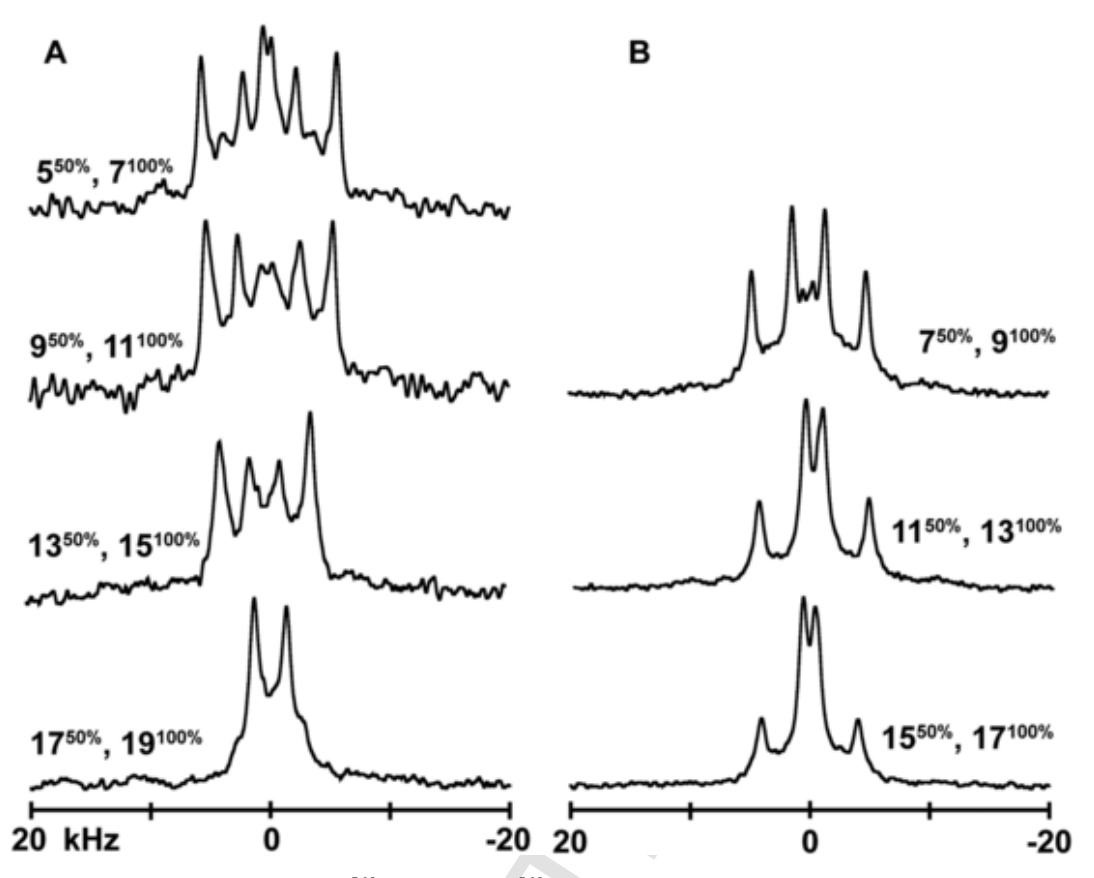


Fig. 2. Deuterium NMR spectra for labeled core alanines of (A) RA $^{5,19}$ ALP23 and (B) RW $^{5,19}$ ALP23 in oriented bilayers of DOPC. The locations and abundance of the  $^2$ H labels are indicated.  $\beta=90^\circ$  sample orientation; temperature 50 °C.

 $\begin{tabular}{ll} \textbf{Table 2} \\ \textbf{Observed} \ ^2 \textbf{H} \ quadrupolar \ splitting \ magnitudes} \ (|\Delta\nu_q|)^a \ \ of \ Ala \ methyl \ side \ chain \ for \ RW \ ^{5,19} ALP23 \ and \ RA \ ^{5,19} ALP23 \ in \ three \ lipids \ ^a. \end{tabular}$ 

| Alanine residue | DLPC                   | DLPC                                |                        |                             | DOPC                   |                             |  |  |
|-----------------|------------------------|-------------------------------------|------------------------|-----------------------------|------------------------|-----------------------------|--|--|
|                 | RA <sup>5,19</sup> ALP | RW <sup>5,19</sup> ALP <sup>b</sup> | RA <sup>5,19</sup> ALP | RW $^{5,19}$ ALP $^{\rm b}$ | RA <sup>5,19</sup> ALP | RW $^{5,19}$ ALP $^{\rm b}$ |  |  |
| 5               | 27.8 ± 1 kHz           | - ( ) =                             | 18.3                   | _                           | 8.8                    | _                           |  |  |
| 7               | 31.0                   | 25.7                                | 28.2                   | 25.7                        | 22.7                   | 18.7                        |  |  |
| 9               | 34.5                   | 28.9                                | 21.7                   | 16.9                        | 10.4                   | 4.7                         |  |  |
| 11              | 29.9                   | 29.0                                | 25.6                   | 24.8                        | 21.1                   | 18.3                        |  |  |
| 13              | 22.2                   | 17.2                                | 12.8                   | 10.4                        | 5.1                    | 3.0                         |  |  |
| 15              | 22.2                   | 22.4                                | 19.0                   | 19.3                        | 15.1                   | 16.2                        |  |  |
| 17              | 7.4                    | 4.0                                 | 4.9                    | 3.0                         | 5.2                    | 2.4                         |  |  |
| 19              | 2.2                    | -                                   | 4.9                    | _                           | 5.2                    | _                           |  |  |
| 3               | 27.1                   | 26.6 °                              | 24.3                   | 24.2 °                      | 20.1                   | 20.4 °                      |  |  |
| 21              | 18.9                   | 14.9 °                              | 16.6                   | 12.5 °                      | 14.5                   | 8.2 °                       |  |  |

a Quadrupolar splittings are reported in kHz for the  $\beta=0^\circ$  sample orientation for RA  $^{5,19}$ ALP and RW  $^{5,19}$ ALP. Each value (in kHz) is the average of the magnitude observed at  $\beta=0^\circ$  and twice the magnitude observed for a  $\beta=90^\circ$  sample orientation. The estimated uncertainty from duplicate samples is  $\pm$  1 kHz. Values not listed (–) were not recorded.

indicates that the helix properties are dominated by the arginine residues, R2 and R22. The tryptophan residues in RWALP23 appear to neither increase nor decrease the extent of the dynamic averaging. The modified Gaussian analysis shows general agreement in predicting once again moderate dynamic averaging, indicated by the  $\sigma_{\rho}$  values generally between 30°–50° (Table 3). As is typical [27,33,34], the more detailed treatment of the dynamics goes hand in hand with somewhat higher predictions for the helix tilt (Table 3), with the overall trends remaining intact. The A5 and A19 data points for the RAALP23 helix

were excluded from the GALA calculations and are illustrated next to the wave plots in Fig. 4. The relative proximities of the  $|\Delta\nu_q|$  values for A5 and A19 to a quadrupolar wave reveal continuation or termination of the central helix (see next section). Because the A19 data point is consistent with the core helix in each lipid membrane, we were able to use seven data points for full Gaussian calculations of the RAALP23 helix dynamics (fitting  $\sigma_\tau$  as well as  $\sigma_\rho$ ) in each lipid membrane. These full Gaussian fits are shown alongside the modified Gaussian results in Table 3. The full Gaussian fits confirm that  $\sigma_\tau$  is less than about  $15^\circ$ 

b Values listed are from [14].

 $<sup>^{\</sup>rm c}\,$  Data points for A3 and A21 are newly reported here.

| Peptide                                   | Lipid             | GALA analysis results <sup>b</sup> |      |                 |         | Modified Gaussian analysis results <sup>c</sup> |      |                |                 |         |                       |
|---|-------------------|------------------------------------|------|-----------------|---------|---|------|----------------|-----------------|---------|-----------------------|
|   |                   | τ                                  | ρ    | S <sub>zz</sub> | RMSD    | $\tau_0$  | ρο   | $\sigma_{	au}$ | $\sigma_{\rho}$ | RMSD    | Ref.                  |
| G <sup>2,22</sup> W <sup>5,19</sup> ALP23 | DLPC              | 21°                                | 305° | 0.71            | 0.7 kHz | 23°   | 304° | 15°            | 33°             | 0.7 kHz | [24]                  |
|   | DMPC              | 9°                                 | 311° | 0.89            | 1.1     | 13°   | 308° | 10°            | 42°             | 1.2     | [17]                  |
|   | DOPC              | 6°                                 | 323° | 0.87            | 0.6     | 9°  | 321° | 9°             | 48°             | 0.7     | [24]                  |
| R <sup>2,22</sup> W <sup>5,19</sup> ALP23 | DLPC              | 23°                                | 305° | 0.70            | 1.0     | 23°   | 305° | 15°            | 24°             | 1.1     | [14],<br>this<br>work |
|   | DMPC              | 14°                                | 307° | 0.80            | 0.6     | $22^{\circ}$                                    | 303° | 15°            | 44°             | 1.9     |                       |
|   | DOPC              | 7°                                 | 318° | 0.86            | 0.7     | 13°   | 315° | 15°            | 54°             | 1.1     |                       |
| R <sup>2,22</sup> A <sup>5,19</sup> ALP23 | DLPC              | 27°                                | 302° | 0.73            | 1.2     | 32°   | 300° | 15°            | 32°             | 1.2     | This<br>work          |
|   | DLPC d            |                                    |      |                 |         | 33°   | 299° | 14°            | 34°             | 0.9     | This<br>work          |
|   | DMPC              | 18°                                | 302° | 0.77            | 0.8     | 24°   | 300° | 15°            | 40°             | 0.7     | This<br>work          |
|   | DMPC <sup>d</sup> |                                    |      |                 |         | 20°   | 302° | 12°            | 32°             | 0.7     | This<br>work          |
|   | DOPC              | 11°                                | 302° | 0.81            | 0.6     | 18°   | 299° | 15°            | 52°             | 0.8     | This<br>work          |
|   | DOPC d            |                                    |      |                 |         | 14°   | 301° | 8°             | 44°             | 0.4     | This<br>work          |

 $<sup>^{\</sup>rm a}$  The methods were described previously [24]. The units for RMSD are kHz.

and  $\sigma_\rho$  retains modest values between about  $30^\circ\text{--}45^\circ$  in each lipid membrane. Overall, each of the peptides in Table 1 folds into a transmembrane helix that is significantly tilted and exhibits only a low level of dynamic averaging.

# 3.2. Fraying of RAALP23 and RWALP23

To address the fraying [15] of the N- and C-terminals of RAALP23 and RWALP23, we recorded the <sup>2</sup>H NMR spectra for A3 and A21 for each peptide, labeled with 50% and 100% deuterium respectively (Fig. 3). In all cases, the spectra reveal sharp and distinct <sup>2</sup>H signals for each

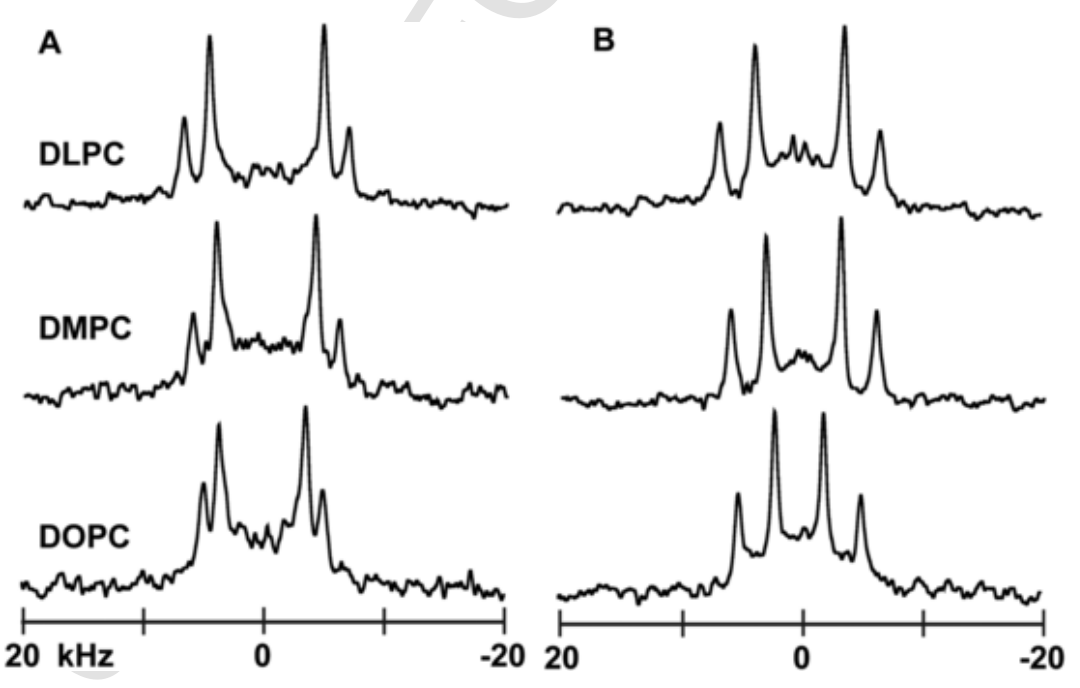


Fig. 3.  $^{2}$ H NMR spectra for the labeled juxta-terminal alanines A3 (50%  $d_{4}$ ) and A21 (100%  $d_{4}$ ) in (A) RA $^{5,19}$ ALP23 and (B) RW $^{5,19}$ ALP23, in oriented bilayers of DLPC, DMPC and DOPC.  $\beta = 90^{\circ}$  sample orientation; temperature 50  $^{\circ}$ C.

b The semi-static GALA analysis [18] was based on the <sup>2</sup>H quadrupolar splitting magnitudes for the six central alanine side chains of residues A7, A9, A11, A13, A15 and A17.

 $<sup>^{</sup>c}$  Unless otherwise noted, the modified Gaussian analysis was based on the  $^{2}$ H quadrupolar splitting magnitudes for the six central alanine side chains of residues A7, A9, A11, A13, A15 and A17 [24,27]; with  $\sigma_{\tau}$  being assigned the fixed value noted in the table and  $S_{zz}$  assigned the fixed value of 0.88.

<sup>&</sup>lt;sup>d</sup> A full Gaussian analysis (varying also  $\sigma_t$ ) [27] was performed based on seven data points for deuterated alanines 7, 9, 11, 13, 15, 17 and 19.

of the terminal alanines 3 and 21 in DLPC, DMPC and DOPC. Observations of different  $|\Delta\nu_q|$  values for A3 and A21, separated by 18 residues or five turns of a "perfect" helix in the same sample, imply helix unwinding at one or both ends [15]. Comparing then the quadrupolar splitting magnitudes of A3 and A21 in RAALP23 (Table 2) with the values for the control peptide RWALP23, one observes that the  $^2H$  quadrupolar splitting for the A3 methyl group remains unchanged in all three lipid systems, yet is farther from the helix that contains the tryptophans (Fig. 4). The  $^2H$   $|\Delta\nu_q|$  value for A21 varies when the tryptophans are substituted by alanines, yet remains in all cases away from the quadrupolar wave that is defined by the central helix (Fig. 4). The fraying of the N-terminal appears to be reduced when W5 is absent, while the fraying of the C-terminal appears comparable in both helices.

In RAALP23, the two extra alanine residues (A5 and A19) provide the opportunity to investigate an extended view of the core helix, thereby the onset of fraying at each end. The results will complement those reported recently for the helix of  $A^{4,5}GWALP23$  [17]. To examine this issue, we analyzed the quadrupolar wave plot for the six central deuterated alanines (odd-numbered residues A7 to A17) and overlaid

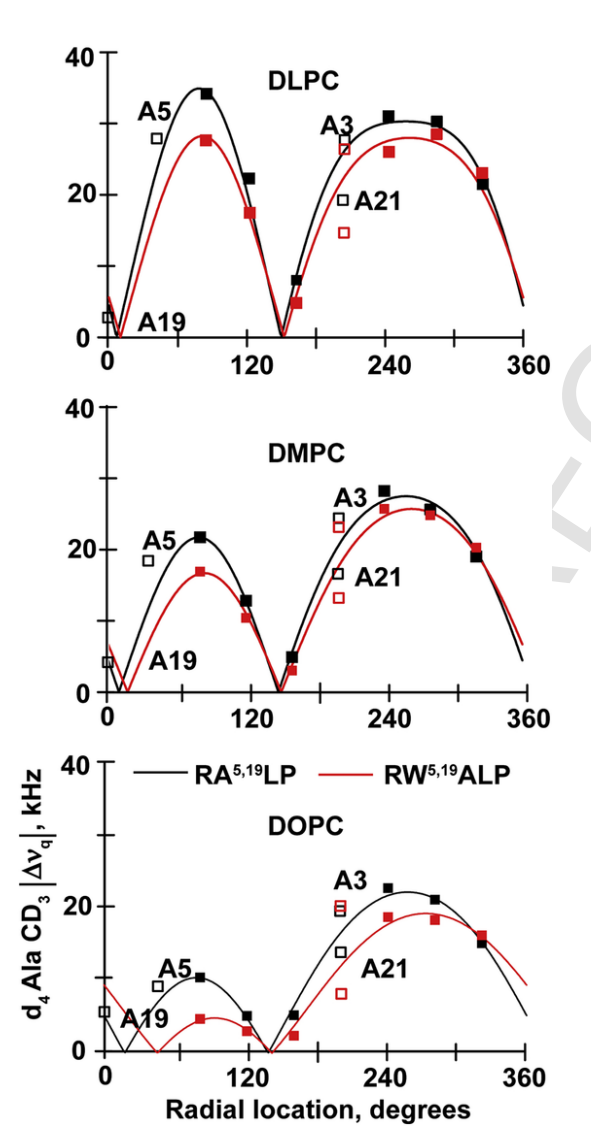


Fig. 4. Quadrupolar wave analysis of tilted transmembrane peptides RA<sup>5,19</sup>ALP23 (black) and RW<sup>5,19</sup>ALP23 (red) in lipid bilayers of DLPC, DMPC and DOPC, as indicated. The  $|\Delta\nu_q|$  values for alanines 3, 5, 19 and 21 were not used in the analytical fits to generate the curves, yet are numbered and shown with open symbols. Residue A19 generally resides closer to the curve for the core helix than residue A3, A5 or A21.

the data points of the remaining four residues A3, A5, A19 and A21 relative to the wave plot (Fig. 4). Importantly, the latter four data points, those outside of the central core, were not used for calculating the quadrupolar wave. It appears that A19 of RAALP23 is essentially integrated into the central helix in all lipid membranes. Indeed, quadrupolar splittings of A19 in DMPC and DOPC are very close to the helical wave and deviate only slightly in DLPC (Fig. 4). On the other hand, residue A5 remains off the helix plot in each lipid bilayer. These results along with those for A3 and A21 (see above) reveal that there is asymmetric fraying of the ends of the helix, with the core helix extending from at least residue 7 to 17 in DLPC, and from 7 to 19 in DMPC and DOPC.

#### 3.3. Deviation of frayed residues from $\alpha$ -helix

Knowing that the peptide termini are unwound involving at least 3 to 5 residues on each side of the central helix, next one can examine and compare the extent of fraying for each end of the RAALP23 and RWALP23 transmembrane helices. The histograms in Fig. 5 show the deviations of residues A3, A5, A19 and A21 from a theoretically "perfect" helix. From the histograms for the outer alanines 3 and 21 in Fig. 5, it is evident that the deviation of A3 from the core helix of either RAALP23 or RWALP23, does not follow the actual tilted transmembrane orientation of the helix in bilayers of different thickness, contrary to the observations for GWALP23 [17]. Rather, A3 is more unraveled when the helices are less tilted, with maximum deviation in the thickest DOPC membrane. The deviations of A3 from the core helix are larger when tryptophan residues W5 and W19 are present (Fig. 5). In RAALP23, observations are available also for A5. Residue A5 follows a different scenario, with the magnitude of deviation from the central helix decreasing gradually when the helix is moved from thinner to thicker lipid membranes.

While the  $|\Delta\nu_q|$  magnitudes for residue A3 are higher than the values predicted from the central helix (Fig. 5), those for residue A21 are lower. This opposite trend for the C-terminal compared to the N-terminal residues has been observed previously for a number of transmembrane helices [17]. One notes further that residue A19 is essentially on the central helix in DOPC and DMPC, while slightly displaced in DLPC (Fig. 5). Residue A21 behaves similarly whether A19 or W19 is present (Fig. 5) and is maximally displaced in DLPC, where the helices adopt the highest tilt from the bilayer normal. By contrast, when arginines are absent, in the presence of G2, G22, W5 and W19 in GWALP23, the deviation of residue A21 from the core helix is essentially constant in DLPC, DMPC and DOPC membranes [17]. These findings reveal that the divergence of some residues involved in the helix unwinding is lipid dependent for peptides anchored by arginine.

Considering the ensemble of results, we note that even though the quadrupolar splitting values of A3 remain very similar when W5 is replaced by A5 (Table 2), A3 nevertheless is more consistent with the core helix when A5 is present, as opposed to W5 (Fig. 5). At the other end, residue A21 deviates from the core helix to about the same extent, regardless of whether A19 or W19 is present.

# 4. Discussion

We have investigated possibilities for cooperation or competition between interfacial charged and aromatic amino-acid side chains for governing the properties of membrane-spanning helices. While such chemical groups make work together, for example in chemotaxis Tar receptors [9] or Kir6.2 potassium channels [3], the respective protein-lipid interactions are complex. For the model systems under consideration to establish the biophysical groundwork, we find that aspects of both collaboration and competition between Arg and Trp residues may come into play.

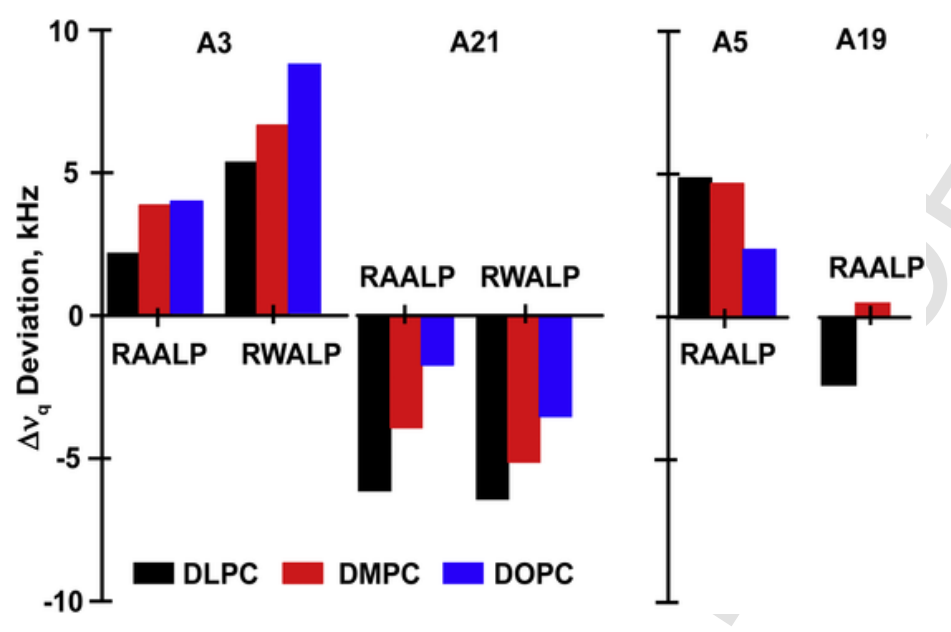


Fig. 5. Deviations of the experimental  $|\Delta\nu_q|$  values for juxta-terminal residues A3, A21, A5 and A19 from the theoretical values fitting the core  $\alpha$ -helix of RA<sup>5,19</sup>ALP23 and RW<sup>5,19</sup>ALP23 in lipid bilayers of different thickness.

Based on considerations of hydrophobic matching and the modulation of lipid phase behavior by Trp-flanked or Lys-flanked peptides of different length, it was revealed that the optimal location for Lys  $(\epsilon \mathrm{NH_3}^+)$  is about 3.4 Å closer to the aqueous phase than that of Trp (NH) [19]. These different "anchoring" positions for Lys and Trp on transmembrane helical peptides validate the choices to investigate the influence and possible interactions of Arg residues (#2 and #22) spaced three positions or about one helical turn outside of Trp residues (#5 and #19) on both ends of a membrane-spanning helix having 23 total residues (Table 1).

The relevance for fundamental biophysical investigations comes from a number of important membrane proteins. The residues flanking a membrane-spanning helix are important for membrane protein assembly and function. For example, a conserved Trp in the Arf and Sar GTPases is located structurally near a myristoylation site and may play a role in membrane association [7]. Tryptophans W491 and W515 flank the single transmembrane domain of a thrombopoietin receptor, for which molecular dynamics simulations suggest that mutations of W515 to leucine or lysine influence the helix tilt angle and rotational distribution [10]. Clinically, some mutations to W515 are associated with thrombocytopenia and myelofibrosis [10]. Such mutations therefore may influence the receptor dimerization propensity and subsequent partner phosphorylation that would influence a signaling cascade related to platelet formation.

Interfacial or embedded arginines also are functionally important for membrane proteins. For example, a notorious central (midspan) arginine in the transmembrane domain of the envelope glycoprotein gp41 of HIV causes water defects in lipid-bilayer membranes [5,6]. These defects seem to be crucial for viral fusion and infection and are relieved if the critical Arg is mutated to Leu [5]. The midspan arginine is perhaps held in place because of strong stabilizing interactions for additional interfacial arginines that flank the defect-causing transmembrane helix of gp41 [6]. In another case, a mutation from Gly to Arg, G805R, in the transmembrane domain of the low-density lipoprotein receptor causes familial hypercholesterolemia, by destabilizing the receptor and causing ectodomain cleavage while preventing  $\gamma$ -secretase cleavage [8]. The effects may relate to a less efficient incorporation of the receptor protein in the endoplasmic reticulum membrane [8].

Sometimes Trp and Arg may act together. The transmembrane signaling domain of the *E. coli* Tar receptor consists of a hydrophobic helical core of QLAVIALVVVLILLVA flanked by tryptophan on each end and then by outer arginines four residues away from each Trp [9]. Notably the design of the Tar receptor helix is similar to the model helices used for our experiments (see Table 1). Mutations of either Trp or Arg influence the piston-like signaling mediated by the Tar helix to activate a downstream kinase [9]. Likewise, two conserved residues, interfacial and interacting Trp and Lys from adjacent transmembrane helices, govern the kinetics of ATP-dependent gating of inward-rectifying Kir6.2 potassium channels [3]. These and other examples illustrate the biophysical importance of interfacial aromatic and charged residues for membrane protein function.

Notably, Trp and Arg differ in their side-chain conformational freedom. The tryptophans are more restricted and, in particular, the N-terminal and C-terminal tryptophans are impacted differently by the  $\alpha$ -helix. The Trp  $C_{\alpha}\text{-}C_{\beta}$  bond is directed toward the N-terminal at an angle of  ${\sim}58^{\circ}$  [18]. Therefore, while the  $C_{\alpha}\text{-}C_{\beta}$  bond orientation inherently directs the N—H bond of an indole ring near the N-terminal of a transmembrane helix toward the bilayer surface, indole rings near the C-terminal must reorient to achieve optimal surface hydrogen-bonding propensity for their Ne-H groups [35]. The preferred sets of  $(\chi 1, \chi 2)$ torsion angles therefore differ for N-terminal and C-terminal Trps on a transmembrane helix, with  $\chi 1$  commonly observed near 180° for the C-terminal Trps but near 60° for the N-terminal Trps. Importantly, as a corollary, Trps near the C-terminal also experience much more motional freedom than those near the N-terminal [35]. These differences are likely responsible for the distinct observation that W19 is more important than W5 for defining the transmembrane properties of the archetypical GWALP23 helix [36]. Key differences are observed also for tryptophans and consequences of Trp replacement at the two end of the Tar receptor helix [9]. The torsional contrasts for Arg arise when comparing surface-located and partially buried Arg residues. Arginine is able to use many torsions to "snorkel" and effectively lengthen or shorten the effective "reach" of its side chain [37-39]. The snorkeling is likely to be important for arginines that are somewhat submerged in a lipid bilayer [5,11,40] but less important for arginines at a membrane surface, such as those considered in the present experiments. Arg and Trp both prefer the membrane interface over the membrane interior, but the arginine preference is stronger. While tryptophan may be relatively well tolerated near the bilayer center [17], arginine is not. Notably, a bilayer-embedded arginine will tend to exit the membrane [11,40] or, if stabilized, will induce a water defect [5,6].

With the above background and knowledge of the preferred interfacial locations for Trp and Arg [19], we have compared in detail the properties of helices having Trp only (G<sup>2,22</sup>W<sup>5,19</sup>ALP23) with no arginines, Arg only (R<sup>2,22</sup>A<sup>5,19</sup>ALP23) with no tryptophans, or Trp and Arg together (R<sup>2,22</sup>W<sup>5,19</sup>ALP23) at the membrane interfaces. The salient trends (Table 3) for this family of helices are these: Each helix displays a relatively low tilt angle from the DOPC bilayer normal; the tilt increases in the thinner DMPC and DLPC bilayer membranes. The trend follows the diminishing membrane hydrophobic thickness, from about 26.2 Å for DOPC at 45 °C [41] to about 24.8 Å and 20.8 Å, respectively, for DMPC and DLPC at 50 °C [42]. When the interfacial tryptophans (W5 and W19) are removed, the helix tilt increases by about 3-4° in each membrane. The preferred helix azimuthal rotation angle and the low extent of dynamic averaging are essentially constant among all helices from Table 1 in all membranes that were investigated. Remarkably, the removal of R2 and R22, or of W5 and W19, does not influence the preferred azimuthal rotation about the helix axis. Graded trends are seen for the unwinding of helix terminals, such that residues 5 and 19 are relatively close to continuations of the central helix, while residues 3 and 21 are notably unraveled.

The trends for the helix tilt support the concept of hydrophobic matching. When tryptophan is removed, the helix tilt increases in each membrane (Table 3), yet the trend for increasing the tilt in the thinner bilayers remains in place. Indeed, for each of the helices, the tilt from the bilayer normal increases by about  $7^\circ$  when moving from DOPC to DMPC, and by an additional  $\sim 9^\circ$  when moving from DMPC to DLPC (Table 3). These results support early concepts for the "matching" of helix hydrophobic length to bilayer membrane hydrophobic thickness [13].

The preferred azimuthal rotation about the helix axis, relative to an arbitrary reference point designated by residue G1, [18] remains remarkably constant for each helix in each bilayer membrane (Table 3). The constancy of the helix rotation may seem surprising, yet may also reflect the "compatible" radial locations of the Arg and Trp residues that are substituted when varying these peptide sequences (Table 1). Indeed, the respective Arg and Trp residues occupy similar radial locations and are spaced from the bilayer center according to their known energetic preferences at a membrane interface [19]. Therefore, in retrospect, it is not so surprising that the helix rotational choices remain similar when Arg is replaced by Gly or when Trp is replaced by Ala. Namely, R2, R22, W5 and W19 are each compatible with a highly similar azimuthal rotation about the axis of the tilted transmembrane helix (Table 3). Furthermore, within this rotational context, the dynamic rotational "slippage"  $(\sigma_0$  in Table 3) about the helix axis remains low in all of the cases tested here. Again, we attribute these features to the compatible "anchoring" locations for either Trp or Arg, or Trp and Arg together, at the membrane interface.

The terminals of all helices are unwound, exposing peptide backbone groups for intermolecular hydrogen bonding with head groups or water at the membrane interface. This feature of transmembrane helix unraveling has been postulated to help stabilize particular helix orientations and limit the dynamics [15]. The examples observed here continue a similar theme. Interestingly, residue A3 deviates from the core helix to a greater extent (kHz deviation of the  $^2H\ |\Delta\nu_q|)$  when W5 is present instead of A5, whereas residue A21 behaves about the same with W19 or A19 (Fig. 5). Nevertheless, when the tryptophans are absent, residue A19 is essentially on the core helix, whereas residue A5 shows a significant deviation (Fig. 5).

In an overall sense, there is a strong expectation that particular arginines will dominate the scene and dictate the helix properties [11].

While the expectation is largely borne out, we note nevertheless that the parent GWALP23 helix exhibits only minor dynamic averaging when Arg is absent. Indeed, it appears that buried or submerged Arg residues dominate more than do interfacial Arg residues at a lipid membrane surface. The interfacial Trp residues furthermore retain their importance. When Arg is absent, the Trp residues are crucial for the properties of the parent GWALP23 helix. In the presence of R2 and R22, the interfacial Trp residues fine tune the helix properties (Table 3; Fig. 4). Our findings confirm that aromatic and charged interfacial side chains are important for the biophysical properties of membrane proteins.

#### Transparency document

The Transparency document associated this article can be found, in online version.

# **Declaration of competing interest**

The authors declare no conflict of interest.

#### Acknowledgments

This work was supported in part by the U.S. National Science Foundation (NSF) Molecular and Cellular Biosciences grant 1713242, the Arkansas Biosciences Institute, and the University of Arkansas Honors College. The peptide, NMR, and mass spectrometry facilities were supported in part by the U.S. National Institutes of Health (NIH) grant GM103429.

# Appendix A. Supplementary data

Mass spectrum, circular dichroism spectra, <sup>31</sup>P NMR and <sup>2</sup>H NMR spectra. Supplementary data to this article can be found online at https://doi.org/10.1016/j.bbamem.2019.183134.

#### References

- M.J. McKay, F. Afrose, R.E. Koeppe 2nd, D.V. Greathouse, Helix formation and stability in membranes, Biochim. Biophys. Acta Biomembr. 1860 (2018) 2108–2117.
- [2] Y. Mokrab, M.S.P. Sansom, Interaction of diverse voltage sensor homo logs with lipid bilayers revealed by self-assembly simulations, Biophys. J. 100 (2011) 875–884
- [3] R.S. Zhang, J.D. Wright, S.A. Pless, J.J. Nunez, R.Y. Kim, J.B.W. Li, R.Y. Yang, C.A. Ahern, H.T. Kurata, A conserved residue cluster that governs kinetics of ATP-dependent gating of kir6.2 potassium channels, J. Biol. Chem. 290 (2015) 15450–15461.
- [4] M. Raja, R.K.H. Kinne, Pathogenic mutations causing glucose transport defects in glut1 transporter: the role of intermolecular forces in protein structure-function, Biophys. Chem. 200 (2015) 9–17.
- [5] M.K. Baker, V.K. Gangupomu, C.F. Abrams, Characterization of the water defect at the HIV-1 gp41 membrane spanning domain in bilayers with and without cholesterol using molecular simulations, Biochim. Biophys. Acta Biomembr. 1838 (2014) 1396–1405.
- [6] L.R. Hollingsworth, J.A. Lemkul, D.R. Bevan, A.M. Brown, HIV-1 env gp41 transmembrane domain dynamics are modulated by lipid, water, and ion interactions, Biophys. J. 115 (2018) 84–94.
- [7] A.F. Neuwald, Bayesian classification of residues associated with protein functional divergence: Arf and arf-like GTPases, Biol. Direct 5 (2010).
- [8] T.B. Strom, K. Tveten, J.K. Laerdahl, T.P. Leren, Mutation g805r in the transmembrane domain of the LDL receptor gene causes familial hypercholesterolemia by inducing ectodomain cleavage of the LDL receptor in the endoplasmic reticulum, FEBS Open Bio 4 (2014) 321–327.
- [9] B.A. Hall, J.P. Armitage, M.S.P. Sansom, Transmembrane helix dynamics of bacterial chemoreceptors supports a piston model of signalling, PLoS Comput. Biol. 7 (2011).
- [10] T.S. Lee, H. Kantarjian, W.L. Ma, C.H. Yeh, F. Giles, M. Albitar, Effects of clinically relevant MPL mutations in the transmembrane domain revealed at the atomic level through computational modeling, PLoS One 6 (2011).
- [11] V.V. Vostrikov, B.A. Hall, D.V. Greathouse, R.E. Koeppe 2nd, M.S. Sansom, Changes in transmembrane helix alignment by arginine residues revealed by solid-state NMR experiments and coarse-grained md simulations, J. Am. Chem. Soc. 132 (2010) 5803–5811.
- [12] V.V. Vostrikov, C.V. Grant, A.E. Daily, S.J. Opella, R.E. Koeppe 2nd, Comparison of "polarization inversion with spin exchange at magic angle" and "geometric analysis

- of labeled alanines" methods for transmembrane helix alignment, J. Am. Chem. Soc.  $130\ (2008)\ 12584-12585.$
- [13] J.A. Killian, I. Salemink, M.R. De Planque, G. Lindblom, R.E. Koeppe II, D.V. Greathouse, Induction of non-bilayer structures in diacylphosphatidylcholine model membranes by transmembrane  $\alpha$ -helical peptides. Importance of hydrophobic mismatch and proposed role of tryptophans, Biochemistry 35 (1996) 1037–1045.
- [14] V.V. Vostrikov, A.E. Daily, D.V. Greathouse, R.E. Koeppe 2nd, Charged or aromatic anchor residue dependence of transmembrane peptide tilt, J. Biol. Chem. 285 (2010) 31723–31730.
- [15] A. Mortazavi, V. Rajagopalan, K.A. Sparks, D.V. Greathouse, R.E. Koeppe II, Juxta-terminal helix unwinding as a stabilizing factor to modulate the dynamics of transmembrane helices, ChemBioChem 17 (2016) 462–465.
- [16] M. Schiffer, C.H. Chang, F.J. Stevens, The functions of tryptophan residues in membrane proteins, Protein Eng. 5 (1992) 213–214.
- [17] F. Afrose, M.J. McKay, A. Mortazavi, V. Suresh Kumar, D.V. Greathouse, R.E. Koeppe 2nd, Transmembrane helix integrity versus fraying to expose hydrogen bonds at a membrane-water interface, Biochemistry 58 (2019) 633–645.
- [18] P.C. van der Wel, E. Strandberg, J.A. Killian, R.E. Koeppe 2nd, Geometry and intrinsic tilt of a tryptophan-anchored transmembrane alpha-helix determined by (2)H NMR, Biophys. J. 83 (2002) 1479–1488.
- [19] M.R.R. de Planque, J.A.W. Kruijtzer, R.M.J. Liskamp, D. Marsh, D.V. Greathouse, R.E. Koeppe, B. de Kruijff, J.A. Killian, Different membrane anchoring positions of tryptophan and lysine in synthetic transmembrane alpha-helical peptides, J. Biol. Chem. 274 (1999) 20839–20846.
- [20] W.L. DeLano, The PyMOL molecular graphics system, The PyMOL Molecular Graphics System, Delano Scientific, San Carlos, CA, 2002.
- [21] P.B.W. Kortenaar, B.G. Dijk, J.M. Peeters, B.J. Raagen, P.J. Adams, G.I. Tesser, Rapid and efficient method for the preparation of Fmoc-amino acids starting from 9-fluorenylmethanol, Int. J. Pept. Protein Res. 27 (1986) 398–400.
- [22] D.V. Greathouse, R.E. Koeppe II, L.L. Providence, S. Shobana, O.S. Andersen, Design and characterization of gramicidin channels, Methods Enzymol. 294 (1999) 525–550
- [23] N.J. Gleason, V.V. Vostrikov, D.V. Greathouse, C.V. Grant, S.J. Opella, R.E. Koeppe 2nd, Tyrosine replacing tryptophan as an anchor in GWALP peptides, Biochemistry 51 (2012) 2044–2053.
- [24] K.A. Sparks, N.J. Gleason, R. Gist, R. Langston, D.V. Greathouse, R.E. Koeppe 2nd, Comparisons of interfacial Phe, Tyr, and Trp residues as determinants of orientation and dynamics for GWALP transmembrane peptides, Biochemistry 53 (2014) 3637–3645.
- [25] J.H. Davis, K.R. Jeffrey, M.I. Valic, M. Bloom, T.P. Higgs, Quadrupolar echo deuteron magnetic resonance spectroscopy in ordered hydrocarbon chains, Chem. Phys. Lett. (1976) 390–394.
- [26] E. Strandberg, S. Ozdirekcan, D.T.S. Rijkers, P.C.A. van der Wel, R.E. Koeppe, R.M.J. Liskamp, J.A. Killian, Tilt angles of transmembrane model peptides in ori-

- ented and non-oriented lipid bilayers as determined by H-2 solid-state NMR, Biophys. J. 86 (2004) 3709-3721.
- [27] E. Strandberg, S. Esteban-Martin, A.S. Ulrich, J. Salgado, Hydrophobic mismatch of mobile transmembrane helices: merging theory and experiments, Biochim. Biophys. Acta 1818 (2012) 1242–1249.
- [28] T.W. Allen, Modeling charged protein side chains in lipid membranes, J. Gen. Physiol. 130 (2007) 237–240.
- [29] B. Roux, Lonely arginine seeks friendly environment, J. Gen. Physiol. 130 (2007) 233–236.
- [30] J.L. MacCallum, W.F. Bennett, D.P. Tieleman, Distribution of amino acids in a lipid bilayer from computer simulations, Biophys. J. 94 (2008) 3393–3404.
- [31] N.J. Gleason, V.V. Vostrikov, D.V. Greathouse, R.E. Koeppe 2nd, Buried lysine, but not arginine, titrates and alters transmembrane helix tilt, Proc. Natl. Acad. Sci. U. S. A. 110 (2013) 1692–1695.
- [32] J.K. Thibado, A.N. Martfeld, D.V. Greathouse, R.E. Koeppe, Influence of high ph and cholesterol on single arginine-containing transmembrane peptide helices, Biochemistry 55 (2016) 6337–6343.
- [33] E. Strandberg, S. Esteban-Martin, J. Salgado, A.S. Ulrich, Orientation and dynamics of peptides in membranes calculated from 2H-NMR data, Biophys. J. 96 (2009) 3223–3232.
- [34] V.V. Vostrikov, C.V. Grant, S.J. Opella, R.E. Koeppe 2nd, On the combined analysis of (2)H and (1)(5)n/(1)H solid-state NMR data for determination of transmembrane peptide orientation and dynamics, Biophys. J. 101 (2011) 2939–2947.
- [35] P.C.A. van der Wel, N.D. Reed, D.V. Greathouse, R.E. Koeppe, Orientation and motion of tryptophan interfacial anchors in membrane-spanning peptides, Biochemistry 46 (2007) 7514–7524.
- [36] N.J. Gleason, D.V. Greathouse, C.V. Grant, S.J. Opella, R.E. Koeppe II, Single tryptophan and tyrosine comparisons in the N-terminal and C-terminal interface regions of transmembrane GWALP peptides, J. Phys. Chem. B 117 (2013) 13786–13794.
- [37] J.A. Killian, G. von Heijne, How proteins adapt to a membrane–water interface, Trends Biochem. Sci. 25 (2000) 429–434.
- [38] S.C. Lovell, J.M. Word, J.S. Richardson, D.C. Richardson, The penultimate rotamer library, proteins-structure function and, Genetics 40 (2000) 389–408.
- [39] M. Tang, A.J. Waring, M. Hong, Phosphate-mediated arginine insertion into lipid membranes and pore formation by a cationic membrane peptide from solid-state NMR, J. Am. Chem. Soc. 129 (2007) 11438–11446.
- [40] M.J. McKay, R. Fu, D.V. Greathouse, R.E. Koeppe II, Breaking the backbone: central arginine residues induce membrane exit and helix distortions within a dynamic membrane peptide, J. Phys. Chem. B (2019) XX. (in press).
- [41] J. Pan, S. Tristram-Nagle, N. Kucerka, J.F. Nagle, Temperature dependence of structure, bending rigidity, and bilayer interactions of dioleoylphosphatidylcholine bilayers, Biophys. J. 94 (2008) 117–124.
- [42] N. Kucerka, M.P. Nieh, J. Katsaras, Fluid phase lipid areas and bilayer thicknesses of commonly used phosphatidylcholines as a function of temperature, Biochim. Biophys. Acta 1808 (2011) 2761–2771.